

## PACK ICE PRESSURE FORECASTING FOR ARCTIC AND SUB-ARCTIC REGIONS

Razek Abdelnour, George Comfort, Sanjay Singh and Bruce Paterson

Fleet Technology Limited  
311 Legget Drive  
Kanata, Ontario  
K2K 1Z8, Canada  
Phone (613) 592-2830  
Fax: (613) 592-4950  
e-mail: fleet@fleetech.com

### ABSTRACT

A model was developed to forecast the ice pressure within an ice cover. The model calculates also the global forces on structures deployed in the ice cover. The model is based on research data collected during several field measurement projects including pack ice pressure in the southern Beaufort Sea, ice pressure in the nearshore ice zone in Labrador and from instrumented ice booms placed in Lake Erie, Lac St. Pierre and the St. Lawrence River. The ice cover characteristics and the driving forces applied on the cover are required as input for the model. The ice characteristics include the ice concentration and the ice thickness distribution of the various types of ice within the ice cover.

### INTRODUCTION

The subject of this paper is to provide quantitative information regarding pack ice pressure magnitude, and the factors controlling them. This information was considered to be a fundamental requirement to the development of reliable methods and indexes for forecasting pressured ice applied on structures and ships.

The general approach was to compare information on pack ice pressures from the available information sources to the scenarios and mechanisms producing pack ice pressure events, and to the controlling factors and trends observed. In particular, the paper focuses on comparing the forces and pressures generated with the ice and environmental conditions (e.g., ice thickness, ice movements, initial concentration and composition of the ice field, winds, currents, their directions).

### PACK ICE PRESSURE EVENTS

Recently, information has been produced by a number of field projects which has the potential to allow an improvement in the present state-of-the-art. The available information sources include:

- Field measurements of pack ice pressure in the southern Beaufort Sea. Three projects were carried out by measuring the stresses in a

large multiyear ice flow; in 1986, (Croasdale et al, 1986); in 1989 (Comfort et al., 1989, 1990); and in 1991 (Comfort et al, 1991). These were further studied in a number of analysis projects where the ice pressure criteria for which an ice floe will start the formation of ridges was developed (Comfort et al, 1994).

- Field measurements of the stresses in the nearshore ice zone near Cartwright, Labrador in 1993. The measurements were made in the landfast ice between Wolf Islands and the Coastline during a period of 16 days. Some data were also acquired to document key environmental conditions such as ice movements, winds, and ice drifts. This field program was conducted by the Bedford Institute of Oceanography (Prinsenberget al, 1997). The principal stress measured was used to calculate the line loads.
- Field data was collected during the winter of 1994 to obtain ice forces on a 2.6 km long ice boom regularly placed at the mouth of the Niagara River (Abdelnour et al, 1994, 1996, Crissman et al, 1995). During this project, three ice load events occurred in early winter. The ice was driven into the boom, and formed between 1.0 and 1.5 m thick pack ice upstream of the boom, eventually causing the ice to overtop the boom. The forces on the boom during these events were measured. Environmental data were also collected and observations were made with a video camera positioned to obtain a view of most of the boom from the roof of a tall building located less than 2 km away.
- Field measurements were made by the Canadian Coast Guard during the winter of 1995 to obtain ice forces on Yamachiche ice boom, a new 2.4 km long steel boom placed in Lac St. Pierre. Data were also collected on Lavaltrie ice boom (about 30 km upstream) placed in the St. Lawrence River. The results were analysed and presented in Abdelnour et al, (1996).

The combination of the above data sets was useful for developing a more broadly-based, general understanding of pack ice pressures as

they cover a wide range of ice conditions, and contain information regarding both the forces and pressures generated, and the associated ice and environmental conditions.

The prediction of the effect of the pressure on ships is a complex issue for several reasons. A wide range of ships operate in the Gulf of St. Lawrence and the Arctic, and hence, the ice pressure events of concern depend on both the ice-capability of the ship(s) of interest and the pressure magnitude, direction and position of the ship within the pack ice. This issue is presented in Paterson et al, (1997).

**CALCULATION OF PACK ICE PRESSURE LINE LOADS**

Data collected during previous field programs indicate that ridge-building pressures are related to the thickness of the ice from which the ridges were formed, termed the ridge ice thickness (Figure 1). Furthermore, the data suggest that the line load is relatively insensitive to the length of the ridging front, for ridging lengths greater than about 400 m (Comfort et al., 1994, and Comfort et al., 1997).

Croasdale et al., 1992 suggested that the interaction force would increase steadily with the ridge ice thickness raised to a power of 1 to 1.25. This is expected to be appropriate for ridge-building in thin ice where flexural failures are predominant. However, as the ridge ice thickness ice becomes greater, crushing becomes a more dominant part of the process. The equations below, which have this general form, were developed from the database (Figure 1), and used to predict pack ice line loads.

$$LL_{rb} = 100 h^{1.25}, \quad \text{for } h < 2 \text{ m} \dots\dots\dots [1]$$

where:

- LL<sub>rb</sub> = the ridge-building line load, in kN/m
- h = the ice thickness, in m, from which the ridge was formed

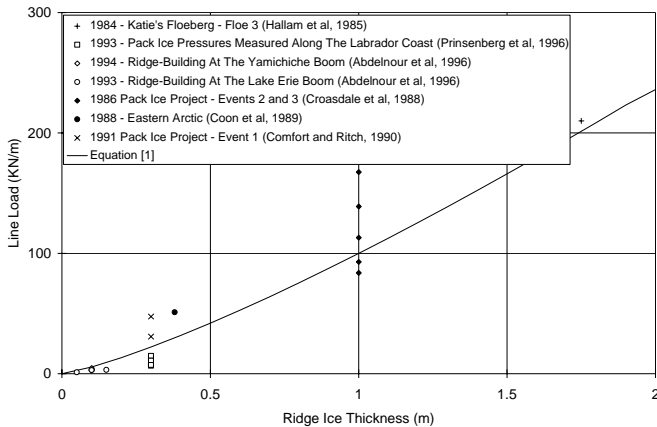


Figure 1: Pack Ice Pressure Line Load

Equation [1] allows the pack ice forces generated during an event to be calculated given that the ridge-building ice thickness is known. The ridge-building thickness, and hence, the ridge-building force is expected to increase during a storm event as ridge-building occurs progressively during an event, starting with the thinnest ice. For these analyses, it was assumed that all of the ice of one thickness in the pack is consumed by ridges before ridge-building shifts to ice of a greater thickness.

Since the ridge building process in ice (thinner than 2 m) is strongly influenced by the ice flexural strength, equation 1 was modified. The effect of the ice thickness and the flexural strength on ridge building forces were examined during a ridge building study carried out at Esso and Arctec ice basins (Graham et al., 1984). Ice sheets ranging from 0.1 m to 0.5 m uniform thickness were prepared and tested at a scale of 1:5 in the Esso basin and at a scale of 1:12 in the Arctec basin. The tests involved towing ice sheets onto an instrumented structure that measured the in-plane force. The structure covered the full width of the basin. A modified relationship where the flexural strength of the ice  $\sigma_f$  is directly related is suggested by assuming the strength of the ice of the data collected is at 700 kPa. The relationship would be as follows:

$$\text{Ice} (< 2 \text{ m}): \quad LL_{rb} = 100 h^{1.25} \text{ for } 700 \text{ kPa} \dots\dots\dots [2]$$

$$LL_{rb} = 0.143 \text{ sf } h^{1.25} \dots\dots\dots [3]$$

**DRIVING FORCES**

The driving forces are generated by winds, wind-waves and currents. The driving force causes the ice to become under pressure when the drifting ice is resisted by the presence of landfast ice, a fixed structure, island, etc. These forces are represented by the following relationship:

$$F_D = F_{wind} + F_{current} + F_{waves} + F_{frontal} + F_{coriolis} \dots\dots\dots [4]$$

where:

- F<sub>D</sub> = Total driving force acting on the ice cover
- F<sub>wind</sub> = Wind force on the ice
- F<sub>current</sub> = Current force on the ice
- F<sub>waves</sub> = Wave force on the ice
- F<sub>frontal</sub> = Frontal force on the ice at the upstream edge of the ice (i.e., Polar Pack)
- F<sub>coriolis</sub> = Coriolis forces

The Polar Pack frontal force exerted on the ice cover is important. However, it depends on the complex movement of the Polar Pack in the Arctic. The Polar Pack force is beyond the scope of this paper. The wave and Coriolis forces exerted on the ice cover is ignored since it is an order of magnitude smaller than the wind and current drag forces. After neglecting some of the forces, the driving force F<sub>D</sub> can be written as:

$$F_D = \tau_c A_c + \tau_w A_w \dots\dots\dots [5]$$

where:

- $\tau_c$  = Current shear stress
- A<sub>c</sub> = Effective ice cover area affected by the current
- $\tau_w$  = Wind shear stress
- A<sub>w</sub> = Effective ice cover area affected by the wind

$$\tau = \rho \cdot g C_d V^2 \dots\dots\dots [6]$$

where:

- $\tau$  = Shear stress ( $\tau_w$  wind,  $\tau_c$  current)
- $\rho$  = Density of water or air (wind  $\rho_w$  and current  $\rho_c$ )
- g = Gravitational acceleration

$C_d$  = Drag coefficient at the air-ice interface  
 $V$  = Velocity of the wind and currents ( $V_w$  and  $V_c$ )

The drag coefficients  $C_{dw}$  for the air-ice and  $C_{dc}$  for the ice-water depend on the roughness which are characterized by Michel (1978). For a rafted ice cover, a value of 0.0033 was selected for the air/ice surface and a value of 0.015 was used for the water/ice surface.

The effective area  $A_c$  onto which the wind and current drag forces are applied on the ice sheet depends considerably on the pack ice interaction scenarios.

A few main scenarios are identified, which apply to most cases seen in nature. These scenarios are depicted from the projects discussed, and are summarized as follows:

**A- Pack Ice Interaction with Coastlines (Very Wide Structures)**

The effective area in this case is equal to the ice fetch along the direction of the driving forces (winds and currents) per unit width. The ice within the fetch should be 10/10 ice concentration to transfer the applied pressures. The field case that applies to this scenario is the Beaufort Sea ridge building project as shown in Figure 2.

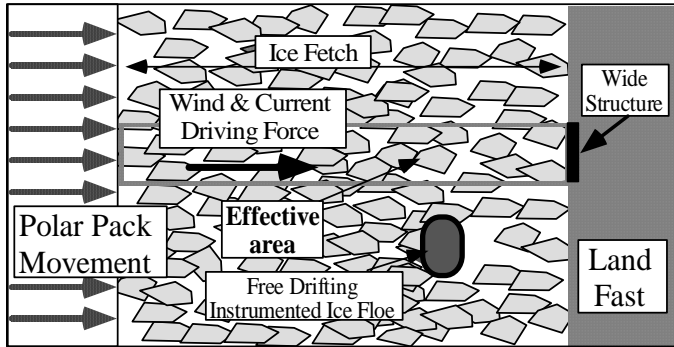


Figure 2: Beaufort Sea Pack Ice Pressure Project

The Lake Erie project is useful in this analysis as long as the accumulated ice upstream the ice boom remains unaffected by the banks of the lake. Figure 3 shows the Lake Erie ice boom. This case applies to a ship beset in ice where the effective area is the ice fetch in the direction of the driving forces that generate the ice pressure.

**B- Pack Ice Interaction with Structures (Very Wide Channel)**

The effective area upstream the structure in a very wide channel  $W \gg B$  has a triangular dead wedge (Figure 4) that have been observed in many studies in the Arctic and river structures (Kovacs et al., 1982; Abdelnour et al, 1995). The dead wedge angle lies between 30 and 70 degrees.

Total force on the structure is the sum of the frictional forces on the sides of the wedge and the wind and the current driving forces on the top and the bottom of the wedge. The forces can be estimated based on earth pressure theories (Terzaghi and Peck, 1967). These

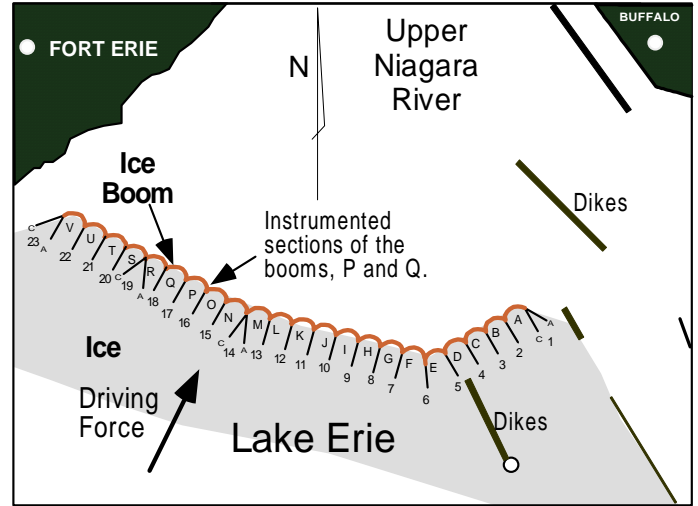


Figure 3: Location of Lake Erie-Niagara River ice boom.

theories show that a dead wedge is formed ahead of the structure. The apex angle of this wedge  $\alpha$  depends on the friction angle  $\phi$  of material and is  $90-\phi$ . Laboratory tests on rubble ice suggest that the friction angle depends on the confining pressure (Ettema and Urroz, 1989). In the case of pack ice, the confinement is produced by the internal pressure of the pack and due to interaction with the landfast ice. Weiss et al. (1981) obtained a friction angle between 10 and 30 degrees at high pressures. For low pressures, the friction angle is between 30 and 60 degrees (Prodanovic, 1979; Urroz and Ettema, 1987).

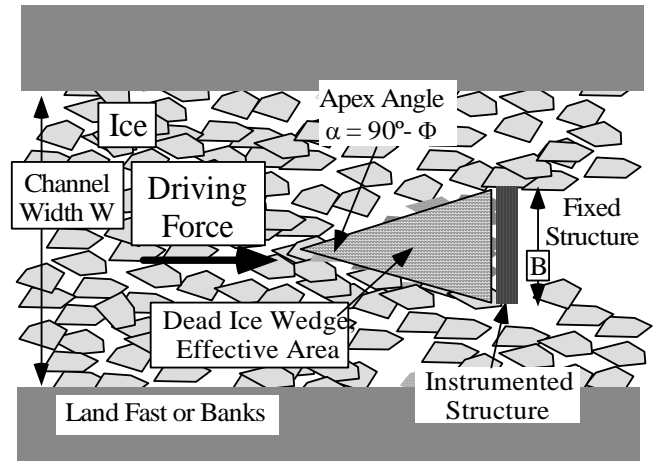


Figure 4: Interaction with Structures

The average line load on the structure can be calculated as:

$$LL = (\tau_c + \tau_w) [ h \{ \tan\phi \cos(45-\phi/2) + \sin(45-\phi/2) \} + 0.25 B \cot(45-\phi/2) ] \dots\dots\dots [7]$$

Where  $h$  is the ice thickness and  $B$  is the width of the structure. For the present analysis, a friction angle of  $\phi = 50$  degrees was used. That is equivalent to an apex angle of  $\alpha = 40$  degrees.

The field case that best fits this scenario is the ice interaction with the St. Lawrence River ice booms. This scenario also applies to moored and fixed offshore structures.

**C- Pack Ice Interaction with a Structure in a Channel**

The effective area upstream of the structure in a narrow channel  $W = B$  is limited by the arching effect of the ice along the banks of the river (Figure 4).

As the pack ice consists of individual interacting floes, it can be assumed to be a material characterized by Mohr-Coulomb failure criterion. Michel (1978) discussed ice pressure on a structure deployed in a moving ice cover in a river channel based on Caquot theories used for grain flow in a hopper. The maximum line load that ice can exert on a floating barrier before ice bridging upstream is calculated as:

$$LL = C (\tau_c + \tau_w) B \dots\dots\dots [8]$$

where B is the width of the structure and C is a constant that depends on the internal friction of the ice. The determination of the length of the broken ice field that should be considered to calculate the thrust on the structure, does not increase indefinitely and this has been studied by investigators in Russia. Latyshenkoff, (1946) found experimentally that after an unconsolidated cover in a river channel became three to four times longer than the channel width (in the direction upstream from a retaining structure) the load on the structure will reach a constant value.

**D- Pack Ice Interaction Parallel to the Coastlines**

Half a wedge develops when the ice drift direction is normal to an exposed part of the coast or on an island near the coast. The field case that best fits this scenario is the ice stress measurement project of winter 1993, at Cartwright, Labrador, (Figure 5).

In this situation, the ice is confined by the coast from one side only, which reduces the confinement and relieves the ice pressure. The line load is calculated using equation 7.

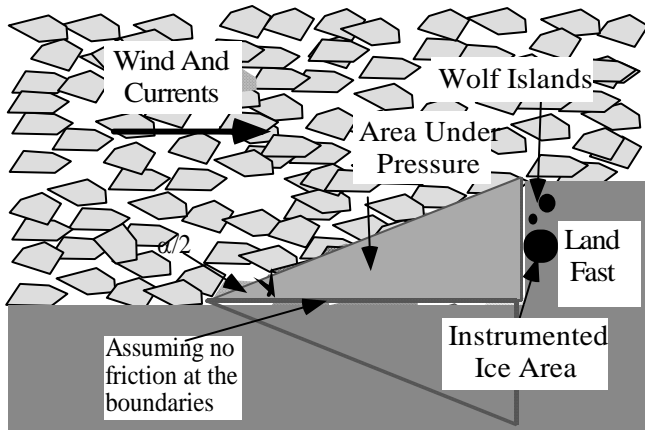


Figure 5: Ice stress measurement project, at Cartwright, Labrador

The ridge building line load of a specific ice cover thickness distribution and strength depends on the driving forces generated by currents and winds and applied on the ice as shown in Figure 6. The higher the driving forces, the more ice is consumed by ridge building and rafting until the driving forces become smaller than the ice resistance to ridge building.

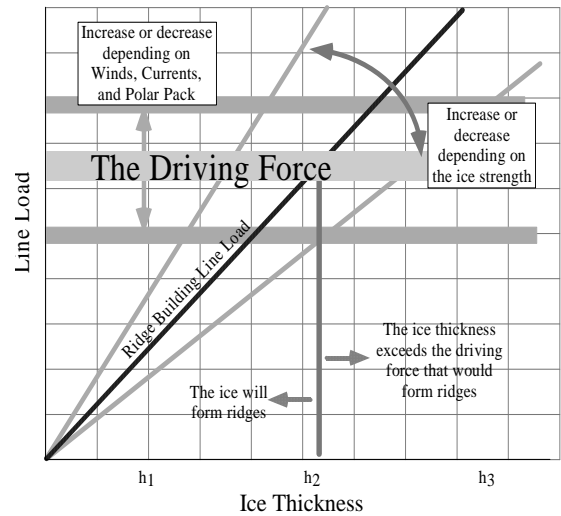


Figure 6: Effect of the Driving Force on the Line Load

**PACK ICE PRESSURE MODEL**

When an ice field is subjected to a converging driving force, the pressure starts to pack the ice to reach higher ice concentration. Depending on the magnitude, duration and the direction of the driving force, the ice may or may not reach complete compaction (i.e., 10/10 ice concentration).

When the ice is completely compacted, the inplane pressure starts to rise until the thinnest ice ( $h_1$ ) within the pack ice starts to fail (see Figure 7). At this time the pressure remains at the same level until all the ice with the thickness ( $h_1$ ) is consumed. Since the ice thickness gradually increases, the effect of ridge building translates into a pressure rise that depends on the ice thickness distribution. If the driving force continues to be larger than the ridge building force, the thicker ice is consumed next. When the driving force becomes equal to the ridge building force, the pressure reaches its ultimate value which is equal to the driving force and no more ice is consumed.

**Ridge Limiting Depth**

The ridge building generates rubble ice that reaches a maximum depth that is directly related to the driving forces. Sayed and Frederking, (1988) developed a model of floating ice rubble pileup to provide the limiting rubble height. The model uses an ice friction  $\phi = 50^\circ$ . The ridge-building load is given by the following relationship:

$$LL_{rb} = 0.76 \gamma_b g H_r^2 = 0.76 (\gamma_w - \gamma_i) (1-p) g H_r^2 \dots\dots\dots [9]$$

Where:

- $LL_{rb}$  = line load (kN/m)
- $H_r$  = limiting ridge depth (m)
- $\gamma_b$  = mass density of bulk rubble or buoyancy of the keel ( $Kg/m^3$ )
- $\gamma_w$  = mass density of water ( $1020 Kg/m^3$ )
- $\gamma_i$  = mass density of ice ( $900 Kg/m^3$ )
- $g$  = gravitational acceleration  $9.81 m/sec^2$ .

p = porosity of the rubble ice, assumed to be 0.2 (Rigby et al, 1976).

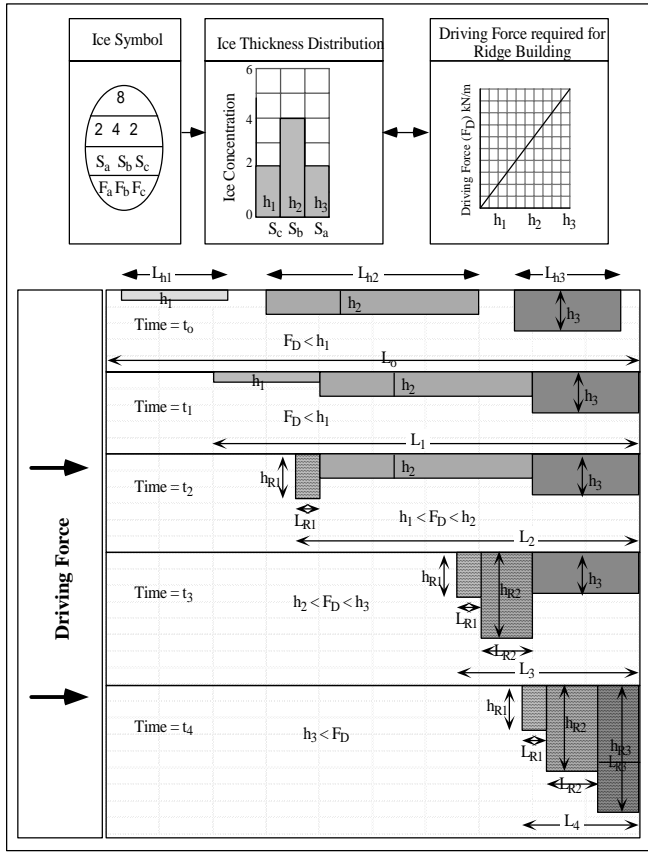


Figure 7: Two-Dimensional Representation of Ice Cover compaction during ridge Building Process

The relationships 4 and 10 can be used to obtain a relationship between the ice thickness and the maximum ridge depth simplified by replacing the constants with the values given above:

$$H_R = 0.45 [\sigma_f h^{1.25} h^{0.5}] \dots\dots\dots [10]$$

The equation 10 gives an upper bound ridge depth which is based on the driving forces that will result in ridge building.

**Pack Ice Compressibility**

When an ice cover with a specific thickness distribution is subjected to a driving force higher than the minimum required ridge building force to fail its thinnest ice, a ridge starts to form. Figure 7 shows a two-dimensional simplification of the ice compaction process.

The thinnest ice  $h_1$  is compacted first to reach a limiting depth of  $H_{R1}$ . The length of the ice cover is reduced from  $L_{h1}$  to  $L_{R1}$ . The volume of ice before and after the compaction process remains constant. A non dimensional pack ice compressibility  $L_{R1}/L_{h1}$  is obtained from the following equation:

$$L_{R1} / L_{h1} = h_1 / [H_{R1} \cdot (1-p)] \dots\dots\dots [11]$$

The value of  $H_{R1}$  in equation 11 is replaced by its value from equation 10 to obtain the following relationship for 700 kPa ice strength:

$$L_{R1} / L_{h1} = h_1 / [(11.9 h_1^{0.625}) \cdot (1-p)] \dots\dots\dots [12]$$

The ice compaction continues if the driving force is larger than the ridge building force with the next ice thickness  $h_2$  and  $h_3$ . The same steps are repeated to calculate  $L_{R2}$  and  $L_{R3}$ .

**Ridge Building Duration**

The time required to compress an ice sheet from its original length  $L_h$  to reach its final length  $L_R$  depends on the driving force and particularly the wind and current speeds normal to the structure. The acceleration and deceleration of the ice is omitted in the proposed model.

From past projects, (1986, 1989 Arctic projects, Labrador experiment, etc.) the drift velocity of the ice due to winds was between 1.2 and 2% of the wind speed. It is expected that during ridge building, this percentage may be smaller since some of the energy will be consumed by the ridge building process in addition to frictional forces. A value of 1% of the wind speed for the ice drift during the ridge building process is considered appropriate.

In currents, the ice drifts at speeds close to 90% of the current speed. However, during ridge building, the ice drift speed is expected to slow down significantly. The value depends on the change in the drag coefficient during the process and the relative current velocity between the ice and the water. A value of 0.5 of the current speed was assumed in this study.

Therefore, in referring to Figure 7, the time required for the ice sheet of thickness  $h_1$  to transform to rubble with a depth of  $H_{R1}$  is given by the following formula:

$$\delta t_1 = t_2 - t_1 = L_{h1} - L_{R1} / [3600 (\alpha W_s + \beta V_s)] \dots\dots\dots [13]$$

Where:

- $t_1$  = time before compaction started (hour)
- $t_2$  = time when compaction was completed (hour)
- $L_{h1}$  = Ice sheet length before compaction started (m)
- $L_{R1}$  = Ice sheet length when compaction was completed (m)
- $W_s$  = Wind speed (m/sec)
- $V_s$  = Current speed (m/sec)
- $\alpha$  = % of wind speed ( $\alpha = 1\%$ )
- $\beta$  = % of current speed ( $\beta = 50\%$ )

Assuming the driving force can build ridges with both ice thicknesses,  $h_1$  and  $h_2$ , the time required to reach a maximum pressure would be  $(t_3 - t_0)$  as shown in Figure 7.

To facilitate the application of the above model, a spreadsheet was setup to calculate the driving force. Based on the ice chart symbol, the spreadsheet calculates the line load required for each ice thickness in the pack to form a ridge, the average ridge height, the resulting pack ice length and the time required to fully compress each ice thickness to transform it into rubble ice. Depending on the scenario of ice pressure, the relationships were programmed to calculate the driving force on an isolated structure, in a channel and along the coastline. The driving force is the ultimate load expected to be reached during the event.

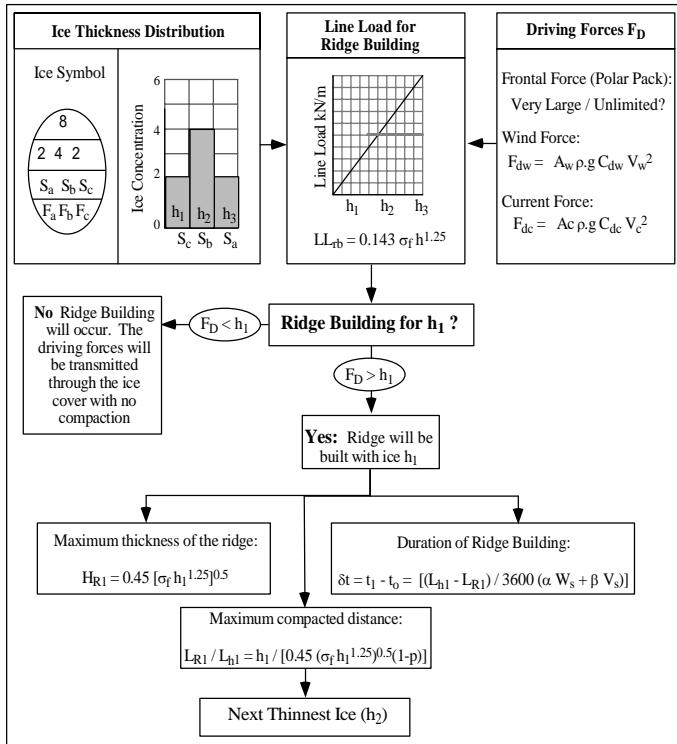


Figure 8: Layout of the Steps Considered for the Pack Ice Pressure

By comparing the driving force to the force required to form ridges, the extent of ridge building and the time required is estimated. Figure 8 presents the steps of the model pack ice pressure calculations.

### ICE PRESSURE CASES

The pack ice pressure model was used to compare with the results obtained from the events measured in the field.

#### Pack Ice Pressure 1986 and 1989 Arctic Events

The pack ice pressure events obtained from an instrumented ice floe in 1986 and in 1989 occurred during the south-west movement of the polar pack ice (see Figure 2). The ice was moving into an area where the distance between the landfast and the polar pack edges was decreasing and generating significant inplane pressure.

The pressure was generated by onshore wind and due to the movement of the polar pack ice. To evaluate the relative importance of each of these two driving forces, the pack ice pressure model was used to obtain the wind driving force.

The ice conditions in the area were obtained from the April 30, 1986 ice chart. The thinnest ice in the ice cover was 120 cm. According to equation 1, the ridge building starts when the line load is in excess of 126 kN/m.

The calculated wind driving force was only 22 kN/m for an average wind speed in the North-South direction of 20 km/hour for the period between April 18 to 22, the days of the two major events.

The line load calculated from the principal stresses measured in a 5 km large ice floe over a period of 22 days recorded significant loads for a period of about 14 hours. During this period, ridge building with ice 1.0 m thick was observed. The calculated line load was 220 kN/m for event 2 and between 120 and 190 kN/m for event 3 (see Figure 1).

It was concluded, that since the measured maximum line load was 220 kN/m, in the pressure range required for ridge building, the polar pack must have been the main driving force. The contribution of the wind to the pressure, 22 kN/m, was of little significance. It should be noted as well that the onshore wind speed was about 10 km/hour for a few days before the event but the measured principal stress was negligible.

The two events measured during the 1989 project confirmed the above findings. However, the second event occurred while the wind speed was 21 km/hour but in the South-North so the wind driving force on the floe should have been zero. The measured line load was 820 kN/m. Ridge building with ice 3 m thick was observed. Therefore, it was concluded that this event was purely due to the polar pack driving force.

#### Pack Ice Pressure, Labrador Coast

Ice stresses in the land fast ice zone was measured during this project. Ice floes were driven by winds and currents and were drifting close to a parallel to the coastline.

The ice conditions in the area were obtained from the March 7, 1993 ice chart, provided by the Canadian Ice Service. The thinnest ice in the ice cover was 30 cm. The ridge building process starts when the driving force reaches a line load of 22 kN/m. Therefore, if any ridge building is to occur, the driving force must be above 22 kN/m.

The line load due to the wind and current driving forces was calculated using equation 7 and by considering half of a triangular shape upstream of the Wolf Islands as shown in Figure 5. The wind normal to the landfast was used as input. The current in the area was considered 0.1 m/sec, deduced from the average drift speed of the ice in the area.

The calculated and measured line are presented in Figure 9. No ridge building is expected to occur since the load was below 22 kN/m. The correlation of the measured and calculated peak loads is within about 20% of the measured loads. The figure shows that the line load measured is close to the ridge building line loads necessary to fail the ice, and not much rafting and ice packing occurred.

An out of phase of about 12 hours is noted between the cycle of the wind and the calculated line load. The model results follow the wind cycle since it is the main driving force. This phase shift is may be due to the time delay caused by the acceleration and deceleration of the ice.

#### Pack Ice Pressure Lake Erie Events

Among the 13 ice pressure events where strong south-west wind events occurred during this project, three are studied here. The ice was driven by winds and currents and was drifting close to the normal direction to an ice boom (see Figure 3).

The wind and current driving forces were calculated for the three events. The ice conditions in the area were obtained from the January 10, 1994 ice chart. The thinnest ice in the ice cover was 10 to 15 cm. According to equation 3, the ridge building process will start when the 10 cm ice starts to fail and when the driving force reaches 3.8 kN/m line load. The line loads obtained for the first three events were 1.2, 3.0 and 3.2 kN/m for events 1 to 3 consecutively. Ice packing occurred in all three events.

The model calculations for the January 8 event were made for the period between 11:00 AM and 3:15 PM. Wind and current input were obtained and are shown in Figure 10. This event provides data that confirms the following:

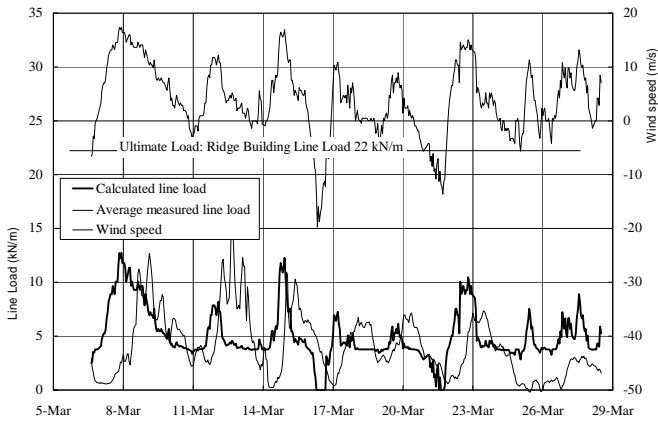


Figure 9: Pack ice pressure, Cartwright, Labrador, 1993

- The calculated line load for ridge building to occur must be at least 3.8 kN/m. The ice packing process occurred on January 8 from 12:00 PM to 3:15 PM. The maximum load measured (before the ice run) over the ice boom was 3.0 kN/m. The calculated line load when full compaction occurred before the ice run was 3.0 kN/m.
- The ridge building duration to compact the ice to 400 m upstream of the boom from an area 800 m upstream of the ice, was approximately 1:15 hours. Using equation 13, the estimated time was 45 minutes.
- The average ridge thickness (HR) that moved over the boom was 1.1 m. The predicted thickness from equation 10 was  $>0.55$  m.
- The compaction ratio was calculated from equation 13 and was 0.20. This means, the 400 m was a result of compacting a one layer thickness of 2000 m. The exact size of the ice cover upstream of the boom was unknown, but it was at least 2000 m.

Pack Ice Pressure, St. Lawrence River Ice Booms

Cable tensions from two ice booms, one deployed yearly in Lac St. Pierre and in the St. Lawrence River near the town of Lavaltrie

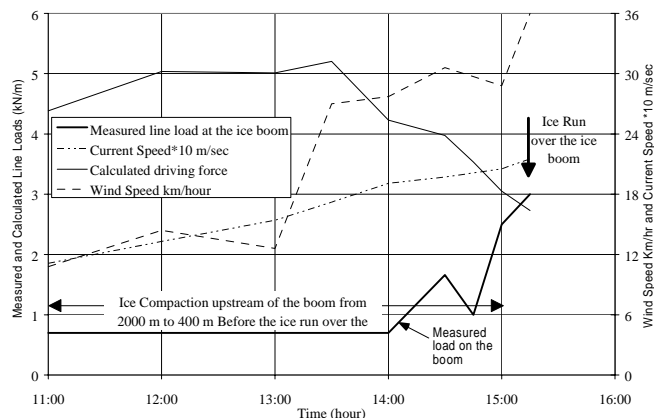


Figure 10: Line Load applied on the Lake Erie Ice Boom - Jan 8, 1993

were collected during the winter of 1994/95. Only the data collected during freeze-up and where ice packing was observed were used.

**Lac St. Pierre, Yamachiche Ice Boom:**

On December 29 the ice started to form and a full pack ice cover was formed by December 31. The calculated line load for the actual wind speed and 0.2 m/sec current is shown in Figure 11.

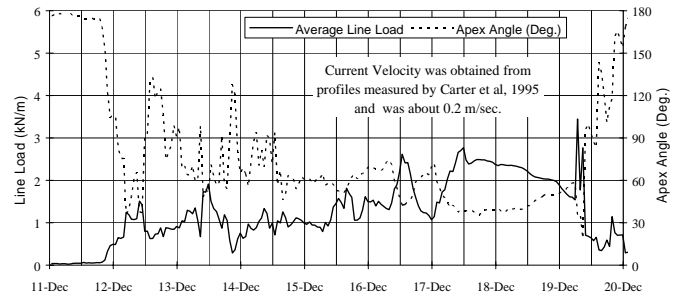


Figure 11: December event, Yamachiche ice boom, Lac St. Pierre

For this case, the scenario in Figure 4 is applicable. In order to evaluate the model proposed in equation 7, the apex angle was calculated from the measured loads. The measured apex angle was between 40 and 60 for the period between December 31 to January 4, 1995 as shown in Figure 11. This range is close to 40°, the value suggested for use in equation 7.

Although a full ice cover formed on December 30 (See Figure 12) the line load did not reach the maximum load until four days later. At the start of the period, the ice cover was 5 to 15 cm thick. Since the calculated ridge building force is 2.4 kN/m (from equation 3), below the driving force of about 3 kN/m, ridge building will occur until all the thin ice is consumed. This was clearly shown in Figure 12.

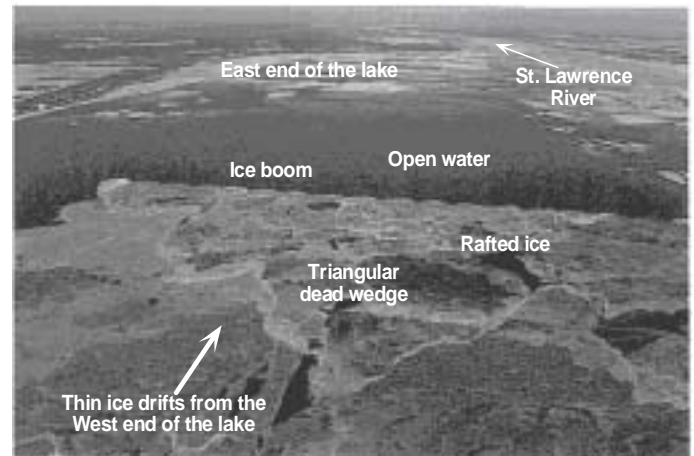


Figure 12: Accumulation of ice upstream of the Yamachiche boom.

**Lavaltrie Ice Boom:**

The ice started to form upstream of the Lavaltrie ice booms on December 29. A full ice cover did not form until a month later. At this ice boom, the driving force (current speed is 0.7 m/sec) is much higher than the capacity of the ice boom. Therefore, the ice was building up upstream of the boom until the load reaches about 4.5 kN/m. At this point the ice runs over the ice boom.

The ice that forms the cover was 5 to 15 cm. The predicted line load for 0.7 m/sec current speed and 25 km/hour wind speed is 16 kN/m. This shows that the load, is by far, larger than the capacity of

the ice boom to retain the ice. The large apex angle maintains the load at 3 to 6 kN/m, the capacity of the ice boom.

## CONCLUSIONS

A simple two-dimensional model (provides thickening of the ice in the vertical plane) to forecast pack ice pressure was developed. The model uses available information currently being gathered by Environment Canada. The calculated line loads, pack ice pressure and its depth obtained using the proposed model compares relatively well to the measured events.

The proposed model is a useful tool to predict the pack ice pressure expected on a structure and a ship transiting between two points. The model requires real-time inputs of the winds, currents and their directions, the ice cover area and their positions.

The usefulness of the model increases with the increase of the ice fetch and the magnitude of the driving forces. For example, for a large ice fetch and a relatively moderate driving force, the pressure require several days to reach its ultimate value. Therefore, for the ultimate pressure to be reached, the wind must persist in the same magnitude and direction for the period.

Part of the model algorithm have been implemented in a simulation model (Comfort et al., 1997) to evaluate the ice loads on an offshore structure deployed in the Beaufort Sea.

## ACKNOWLEDGEMENT

This paper is based on several studies funded during the past ten years. We are particularly grateful to Mr. Randy Crissman, New York Power Authority, Dr. Ibrahim Konuk, National Energy Board, Dr. Brian Morse and Mr. Robert Wolfe, Canadian Coast Guard and Tom Carriere, Canadian Ice Service.

## REFERENCES

- Abdelnour, R., Cowper, B., Gong, Y., H. T. Shen and Comfort, G., 1996, Assessment Of Ice Boom Technology For The Upper Niagara River, Fleet Technology Ltd. Phase II Final Report, No. 4316 Submitted to the New York Power Authority.
- Abdelnour, R., Crissman, R. and Comfort G., 1994, "Assessment of Ice Boom Technology for Application to the Upper Niagara, River.", Proceedings of the IAHR Symposium on Ice Problems, Trondheim.
- Carter, D., Stander, E., and Hodgson, M., 1995, "Technical Assistance, Ice Management in Lac St. Pierre." Report Submitted to Transportation Development Centre, Montreal, PQ, Canada.
- Comfort, G. and Ritch, R., 1989, "Field Measurements Of Pack Ice Stresses", Fleet Technology Ltd. Report 3154 submitted to the Department Of Public Works.
- Comfort, G. and Ritch, R., 1990, "Field Measurements Of Pack Ice Stresses", proceedings. OMAE conference, Houston.
- Comfort, G. and Ritch, R., 1991, "Pack Ice Stress Measurements", Fleet Technology Ltd. Report 3935 submitted to the National Research Council, Canada.
- Comfort, G., Dinovitzer, A., and Gong, Y., 1994, "Limit-Force Ice Loads and their Significance to Offshore Structures in the Beaufort Sea.", prepared by Fleet Technology Limited for the National Research Council, Ottawa, FTL Report 4346C, 1994.
- Comfort, G., Singh, S., and Dinovitzer, A., 1997, "Limit-Force Ice Loads and their Significance to Offshore Structures in the Beaufort Sea.", ISOPE (in Preparations).
- Coon, M.D., Lau, P.A., Bailey, S., and Taylor, B., 1989, Observations Of Floe Stresses In The Eastern Arctic, proc. POAC Conference, Lulea, Sweden.
- Crissman, R., Abdelnour, R., and Shen, H.T. 1995 "Design Alternatives for the Lake Erie-Niagara River Ice Boom." 8th Workshop on River Ice, Kamloop, BC, Canada.
- Croasdale, K., Comfort, G. and Graham, B., 1986, "A Pilot Program to Measure Pack Ice Driving Forces", Report submitted by K.R. Croasdale and Assoc. Ltd. and Fleet Technology Ltd. to the Institute Of Ocean Sciences.
- Croasdale, K., Comfort, G., Frederking, R., Graham, B. and Lewis, L., 1988, "A Pilot Experiment To Measure Arctic Pack Ice Driving Forces", proc. POAC Conference, Fairbanks, Alaska.
- Croasdale, K., Frederking, R., Wright, B., and Comfort, G., 1992, "Size Effect On Pack Ice Driving Forces", proc. IAHR Symposium on Ice Problems, Banff.
- Ettema, R., Urroz, G.E., 1989, "On Internal Friction and Cohesion in Unconsolidated Ice Rubble.", Cold Reg. Sci. Tech., Vol.16.
- Graham B.W., Potter, R.E., Wood, K.N., Comfort, G., 1984, "Rubble - Protected Drilling System Development." Proceedings of the IAHR Symposium on Ice Problems, Hamburg.
- Hallam, S., Duckworth, R, Pickering, J., and Westermann, P., 1985, Katie's Floeberg 1985: Pack Ice Driving Force Measurements, internal British Petroleum report prepared by the Technology Development Division.
- Kovacs, A., Sodhi, D.S., Cox, G.F.N, 1982, "Bering Strait sea ice and the Fairwar Rock Icefoot.", CRREL Report 82-31.
- Latishekov, A.M., 1946, "Investigation of Ice Booms." Hydrotechnic Structures, No. 15:4, USSR
- Michel, B., 1978, "Ice Mechanics." Presse Université Laval, PQ.
- Paterson B, Abdelnour R., Comfort G., Wolfe R., and Carriere T., 1997 "Shipping in Pressurized Ice Conditions: A Preliminary Review." Society of Naval Architects and Marine Engineers Annual Meeting. (In preparation)
- Prinsenber, S. J., Fowler, G. A., Van der Baaren, Beanlands, B., 1997 "Ice Stress Measurements from Land-Fast Ice Along Canada's Labrador Coast." (to appear in Cold Regions Science and Technology Journal).
- Prodanovic, A., 1979, "Model Tests of Ice Rubble Strength.", Proc. POAC 79, Vol. I, Trondheim, Norway, pp. 89-105.
- Sayed M. and Frederking R., 1988, "Model of Ice Rubble Pileup." Journal of Engineering Mechanics, ASCE Vol. 114, pp 149-160.
- Rigby, F. A. and Hanson, A., 1976, "Evolution of a Large Arctic Pressure Ridge.", Aidjex Bulletin, No. 34, Dec., pp 43-71.
- Terzaghi, K., Peck, R. B., 1967, "Soil Mechanics in Engineering Practice.", John Wiley and Sons, Inc.
- Urroz, G. E., Ettema, R., 1987, "Simple Shear Box Experiments with Floating Ice Rubble.", Cold Reg. Sc. Tech., Vol. 14, pp. 185-199.
- Weiss, R. T., Prodanovic, A., "Wood, K. N., 1981, Determination of Ice Rubble Shear Properties.", Proceedings of the IAHR Symposium on Ice Problems, Quebec, Vol. 2, pp. 860-872.